CLASSIFYING STAGES OF CIRRUS LIFE-CYCLE EVOLUTION

Benedikt Urbanek[1]*, Silke Groß[1], Andreas Schäfler[1], Martin Wirth[1]

*[1]Deutsches Zentrum für Luft- und Raumfahrt, Institut für Physik der Atmosphäre, Oberpfaffenhofen , Germany, *benedikt.urbanek@dlr.de*

ABSTRACT

Airborne lidar backscatter data is used to determine in- and out-of-cloud regions. Lidar measurements of water vapor together with model temperature fields are used to calculate relative humidity over ice (RH_i). Based on temperature and RH_i we identify different stages of cirrus evolution: homogeneous and heterogeneous freezing, depositional growth, ice sublimation and sedimentation. We will present our classification scheme and first applications on mid-latitude cirrus clouds.

1 INTRODUCTION

Cirrus clouds are an important constituent of the Earth-atmosphere system. Their radiative properties depend both on macroscopic and microphysical parameters. As knowledge on cirrus clouds is still incomplete, they impose high uncertainties on climate prediction [1]. For instance it is unclear how cirrus properties change, as the cloud evolves in time.

To study possible dependencies on cirrus evolution, we developed a method that identifies regions inside a measured cloud corresponding to different thermodynamic states with regards to cirrus formation, particle growth and sublimation. This is done by evaluating temperature and RH_i, as those two are main parameters determining the thermodynamic state.

In order that ice can form in the atmosphere, RH_i must reach or surpass 100 %. Such areas are called ice-supersaturated regions (ISSR). The existence of an ISSR does not imply the existence or formation of a cirrus cloud. For the homogeneous freezing (HOM) of solution droplets at cirrus temperature (< 235 K), high supersaturations in the order of 140 % are necessary [2]. Additionally, solid aerosol particles can act as ice nuclei and thus lead to freezing under a much broader range of conditions (heterogeneous freezing, HET).

Once ice particles are present, remaining supersaturation is depleted by deposition of water vapor onto existing crystals (DEP). Also regions of subsaturation with respect to ice (SUB) can emerge, when heavy ice particles sediment out of the ISSR or RH_i is reduced by warming, leading to sublimation of ice crystals.

Our method can help to put in-situ and remote sensing data in perspective to cirrus evolution and to investigate the respective optical, microphysical and radiative properties of cirrus clouds.

We present its application in a case study of a lee wave influenced cirrus cloud, obtained during the ML-CIRRUS experiment 2014 and first results from a statistical analysis of cloud optical properties. We also aim to combine our classification with trajectory based methods to reveal information on the temporal development of classified evolution stages

2 METHODOLOGY

2.1 Differential Absorption Lidar WALES

WALES is an airborne lidar that measures the tropospheric water vapor concentration below the aircraft by simultaneously emitting laser pulses at three online and one offline wavelength in the water vapor absorption band around 935 nm [3]. Additionally, WALES features a channel at 1064 nm and one HSRL channel at 532 nm; both, polarization sensitive. An analysis of its accuracy can be found in [4]. WALES

provides collocated measurements of humidity, backscatter ratio (BSR) and aerosol depolarization ratio (ADEP). We calculate RH_i from WALES humidity data and ECMWF analysis and forecast temperature data, that we interpolate both temporally and spatially onto the lidar measurement cross-section (see [5], their Sec. 2).

2.2 ML-CIRRUS campaign

In March and April 2014, the Mid-Latitude Cirrus mission ML-CIRRUS was carried out, designed to investigate natural and traffic induced cirrus clouds. Therefore the German research aircraft HALO was equipped with a combined in-situ and remote sensing payload and performed 16 research flights above Central Europe and the North Atlantic, probing mid-latitude cirrus clouds originating from e.g. air traffic, warm conveyor belts, jet streams, or mountain waves [6].

2.3 Classification scheme

Our classification scheme is outlined in Fig. 1. First a threshold for BSR of 2 is used to determine in- and out-of-cloud regions. Then we employ temperature dependent RH_i thresholds for HOM and HET and a RH_i value of 100 % to distinguish DEP/ISSR and SUB regions. Freezing onset parameterization ($RH_{i,HOM}$, $RH_{i,HET}$) is taken from [2,7].

Outside of clouds, $ISSR_{out}$, HET_{out} and HOM_{out} represent regions of ever more favorable ice nucleation. Inside, HET_{in} and HOM_{in} regions show active ice nucleation. DEP and SUB regions are in a later stage of evolution dominated by crystal growth and ice sublimation.

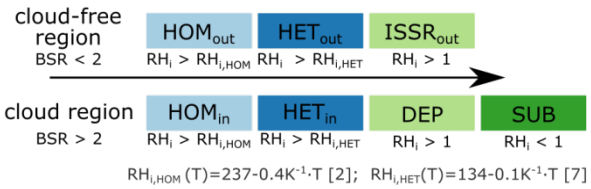

Figure 1: Cirrus evolution classification scheme

3 RESULTS

3.1 Case study ML-CIRRUS 2014-03-29

We apply our classification scheme to a cirrus case that was obtained during ML-CIRRUS on 29 March 2014. A trough, extending from west Ireland to the Iberian Peninsula and further to the western part of North Africa (Fig. 2), leads to high southerly winds with speeds of up to 35 ms^{-1} over Southern France and Spain at 300 hPa.

The flight path (Fig. 2, red) was chosen to run against the main wind direction over Southern France, intersecting a cirrus cloud influenced by the gravity lee wave of the Pyrenees. Our case study focuses on this southward flight leg (Fig. 2 white).

In Fig. 3 a), BSR along the chosen flight leg is plotted. On the lee side, north of the Pyrenees (14:19-13:34 UTC), a high cirrus cloud is observed, with BSR values up to 200, that extends from a height of 7 km to 11 km. ADEP of more than 30 % and temperatures below 240 K (not shown) clearly indicate a pure ice cloud.

Furthermore, in the region between the two clouds (14:34-14:43 UTC) gravity lee waves can be spotted at about 10 km and also in the lower aerosol layer.

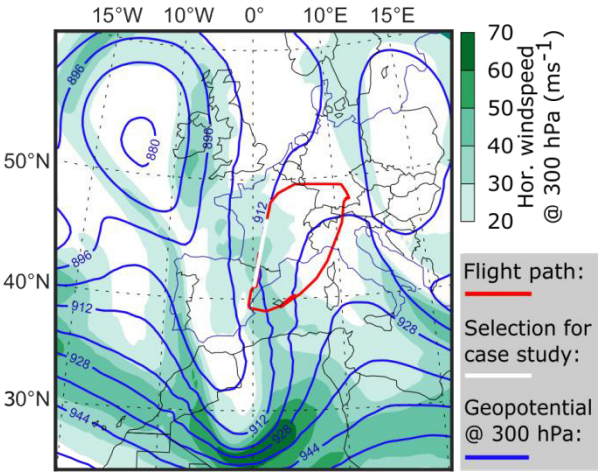

Figure 2: Meteorological situation 2014-03-29

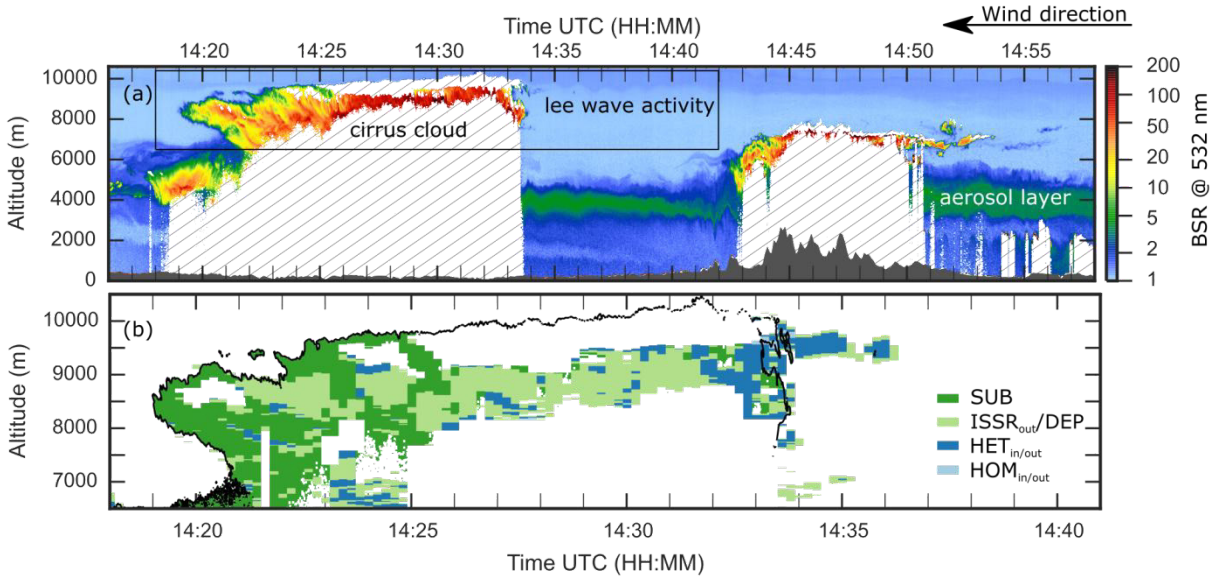

Figure 3: (a) Backscatter ratio at 532 nm cross-section measured by WALES. (b) Visualization of evolution classification, cloud border: black contour line (BSR=2)

Fig. 3 b) shows classified evolution stages. Cloud-free regions and cloud regions can be distinguished by the black contour line for a BSR value of 2.

A humid layer, at about 9.5 km, reaches ice supersaturation (ISSR) in the two crests of the gravity lee wave to the south of the cloud (14:34-14:36 UTC). Here values of RHi are even higher than the threshold for HET freezing. At the cloud edge, also the HOM freezing threshold is surpassed (14:33 UTC). The southern section of the cirrus is dominated by ice nucleation and represents the youngest part of the cloud.

In the middle (14:26-14:32 UTC), a section of moderate supersaturation (DEP) is located. This is an already well developed part of the cirrus that is dominated by depositional growth of ice crystals. After an initial ascent (14:32-14:34 UTC), the cloud top level slopes from over 10 km down to under 9 km at the northern edge. This indicates a large-scale decent reducing supersaturation and evoking the intermediate DEP region as well as large connected areas of subsaturation (SUB) in the northern part of the cloud. Here it is starting to break up, as ice particles are sublimating.

3.2 Statistical Analysis

This classification can also be applied to the complete lidar data set to study optical cirrus properties in a more statistical approach. Fig. 4 shows the distribution of ADEP occurrence during ML-CIRRUS for in-cloud evolution stages. They feature a maximum around 40 % with a tendency towards higher values going from HET to DEP to SUB. SUB also shows a pronounced secondary maximum at 52 %.

Our ongoing research aims to resolve such multimode features by taking other factors

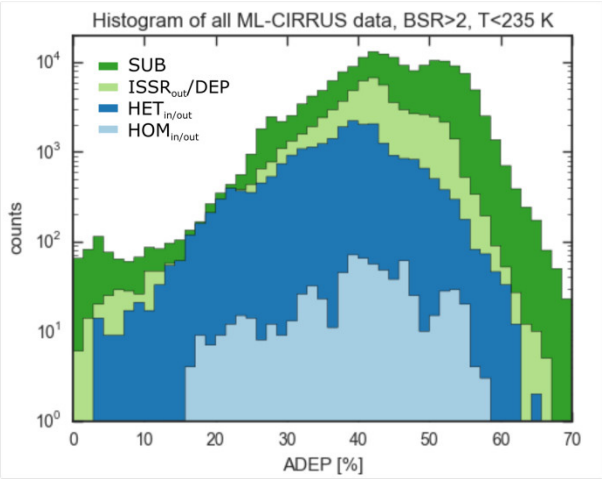

Figure 4: Distribution of Linear Depolarization

into account like cloud type, formation process and meteorological context. Therefore it seems to be promising to also combine this method with results from trajectory based classifications that identify in-situ and liquid-origin cirrus types.

4 CONCLUSIONS

Airborne DIAL water vapor measurements are used together with model temperature data and parameterizations for freezing onset conditions to identify all relevant stages of cirrus cloud evolution. In cloud-free air (BSR < 2), ice supersaturated regions ($ISSR_{out}$) as well as regions of homogeneous (HOM_{out}) and heterogeneous freezing (HET_{out}) are determined. These indicate favorable areas of cirrus cloud formation. Inside the cloud, ice nucleation (HOM_{in}, HET_{in}), depositional growth (DEP) and sublimation regions (SUB) are distinguished, representing the formation, growing and break up phases of a cirrus cloud.

Our method is used to investigate the large airborne lidar data set obtained during ML-CIRRUS. It facilitates the study of the spatial distribution of evolution stages and helps to set in-situ and other remote sensing data in perspective to cirrus evolution. By bringing together those data sources, the specific optical and microphysical properties of different cirrus stages can be explored. Combining our method with trajectory based classifications promises to also reveal details of the temporal succession of evolution stages.

ACKNOWLEDGEMENTS

This work is funded by DLR VO-R young investigator group. The authors like to thank the staff members of the HALO aircraft for preparing and performing the measurement flights, Christiane Voigt, Andreas Minikin and everybody contributing to the successful planning and execution of ML-CIRRUS, and ECMWF for providing model data.

References

[1] Baran, A. J., 2012: From the single-scattering properties of ice crystals to climate prediction: A way forward, *Atmos. Res.,* **112**, 45-69.

[2] Koop, T., B. Lou, A. Tsias, and T. Peter, 2000: Water Activity as the Determinant for Homogeneous Ice Nucleation in Aqueous Solutions, *Nature,* **406**, 61-614.

[3] Wirth, M, A. Fix, P. Mahnke, H. Schwarzer, F. Schrandt, and G. Ehret, 2009: The airborne multi-wavelength water vapor differential absorption lidar WALES: System design and performance, *Appl. Phys. B*, **96**, 201-213.

[4] Kiemle, C. et al., 2008; First airborne water vapor lidar measurements in the tropical upper troposphere and mid- latitudes lower stratosphere: accuracy evaluation and inter-comparisons with other instruments, *Atmos. Chem. Phys*., **8**, 5245-5261.

[5] Urbanek, B., S. Groß, A. Schäfler, and M. Wirth, 2016: Determining stages of cirrus life-cycle evolution: a cloud classification scheme, *Atmos. Meas. Tech. Dis.,* doi:10.5194/amt-2016-332, in review.

[6] Voigt, C., et al., 2016: ML-CIRRUS – The airborne experiment on natural cirrus and contrail cirrus with high-altitude long-range research aircraft HALO, *B. Am. Meteorol. Soc.*, doi:10.1175/BAMS-D-15-00213.1.

[7] Krämer, M., et al., 2016: A microphysics guide to cirrus clouds – Part 1: Cirrus types, *Atmos. Chem. Phys.*, **16**, 3463-3483.